Article type : Original Article

Interactions between rheumatoid arthritis synovial fibroblast migration and endothelial cells

Birgit Zimmermann-Geller[1], Sina Köppert1, Nina Kesel[2], Rebecca Hasseli[1], Sebastian Ullrich[2], Stephanie Lefévre[1], Klaus Frommer[1], Thorsten Gehrke[3], Markus Schönburg[4], Stephan Rehart[5], Udo Schumacher[2], Ulf Müller-Ladner[1], Elena Neumann[1]

1: Department of Internal Medicine and Rheumatology, Justus-Liebig-University Gießen, Campus Kerckhoff, Bad Nauheim, Germany

2: Institute for Anatomy II: Experimental Morphology, University Hospital Hamburg-Eppendorf, Germany

3: Department of Orthopaedic Surgery, Helios ENDO-Klinik Hamburg, Germany

4: Department of Cardiac Surgery; Kerckhoff-Klinik, Bad Nauheim, Germany

5: Department of Orthopedics and Trauma Surgery, Agaplesion Markus Hospital, Frankfurt, Germany

Corresponding author: Dr. Elena Neumann

Justus-Liebig-University Gießen

Campus Kerckhoff-

Benekestr. 2-8

D-61231 Bad Nauheim, Germany

Phone.: +49 (0) 6032 996 2801 Fax: +49 (0) 6032 996 2809

Email: e.neumann@kerckhoff-klinik.de

Key Words: Rheumatoid arthritis, E-selectin, cell migration, fibroblasts

Running head: E-selectin in arthritis

ABSTRACT

Leukocytes travel within the circulation and enter connective tissues by interactions with endothelium of postcapillary venules mediated by cell adhesion molecules, summarized as leukocyte adhesion cascade. In the SCID-mouse-model, rheumatoid arthritis (RA) synovial fibroblasts (SF) migrated to distant cartilage through the vasculature. Therefore, RASF-adhesion towards endothelial cells (EC) and E- and P- selectins were analyzed.

Cell-to-cell-binding assays between SF and EC were performed. Interactions of SF with (TNF-activated) EC or selectins were analyzed in flow-adhesion-assays. Immunohistochemistry for E-selectin-ligand CD15s was performed. CD15s-induction in RASF by human serum or media was evaluated. Wildtype and E-/-/P-/-Select-SCID-mice were used for inverse-wrap surgery. After laser-mediated microdissection, realtime-PCR for E-/P-selectin/VCAM-1 was performed.

Adhesion between SF/EC under static conditions was highest in RPMI-cultured RASF to TNF-activated HUVEC (2.25-fold) and RASF-adhesion was higher towards venous than arterial EC (DMEM $P = 0.0419$, RPMI $P = 0.0119$). In flow-chamber assays, RASF adhesion to E-selectin was higher than to P-selectin (e.g. 0.9 dyn cm^{-2} $P = 0.0001$). OASF showed lower rolling/adhesion properties (e.g. 0.5 dyn cm^{-2} $P = 0.0010$). RASF-adhesion to TNF-activated EC was increased (e.g. 0.9 dyn cm^{-2}, $P = 0.0061$). CD15s-induction in RASF was strongest in RA serum. Vimentin/CD15s double-positive cells were detectable. In E-/P-selectin-deficient mice, contralateral invasion was reduced ($P = 0.023$). E-, P-selectin and VCAM-1 expression in EC of implants was confirmed.

Our data indicate that the milieu within vessels induces CD15s which enables RASF to interact with E-selectin/EC under flow. Therefore, RASF may migrate to distant sites and leave the vasculature similarly to leukocytes.

INTRODUCTION

For their normal function, leukocytes have to leave the bloodstream in order to enter connective tissue spaces where an inflammatory process takes place. Endothelial cells (EC) are activated by inflammatory factors leading to expression of cell adhesion molecules (CAM) on the luminal surface of EC and hence binding of leukocytes to EC via these cell adhesion molecules. Inflammation and synovitis are key features of rheumatoid arthritis (RA) with increased influx of inflammatory cells into affected joints. In addition to leukocytes, synovial fibroblasts (SF) from rheumatoid arthritis (RA) patients were shown to migrate from the original implantation site to human cartilage implanted at a distant site in a severe combined immunodeficient (SCID) mouse model [1, 2]. This migration behavior was unique for RASF and not observed for controls such as SF from osteoarthritis (OA) patients in which chronic autoinflammation is absent. Therefore, specifically preactivated RASF [3-6] seem to interact with EC, presumably via similar mechanisms and molecules as leukocytes. Interestingly,

tumor cells acquire the ability to migrate via the blood stream and to form metastases at distant sites in the body by attaching to endothelial selectins [7, 8]. As it could be shown that migrating tumor cells use the same mechanisms as leukocytes during vascular transmigration [9], we hypothesize that RASF may use similar mechanisms.

During the leukocyte adhesion cascade, different consecutive steps of adhesion to EC are active. The first step is called tethering mediated by attachment via CAM between EC and leukocytes, followed by rolling of leukocytes over the EC layer, slowing down the cells and leading finally to firm attachment to the EC [4, 10]. The first attachment is mediated by selectins and their ligands such as P-selectin glycoprotein ligand-1 (PSGL-1) or Sialyl-Lewis X (CD15s). Then, the rolling leukocytes firmly attach via cell adhesion molecules such as integrins to binding members of the immunoglobulin superfamily on EC such as VCAM1 (vascular cell-adhesion molecule 1) [11]. The firm adhesion between cells is a requirement for the transmigration through the EC layer.

To allow leukocytes to interact with selectins, dynamic flow conditions are required, as selectins can only be bound during shearing forces [12]. If the force is reduced, cells detach from the vessel wall [13]. Selectins belong to the family of CAM. They represent single chain transmembrane glycoproteins which attach to sialylated and fucosylated ligands [14]. E-selectin is expressed on activated EC, P-selectin is present on the surface of platelets and activated EC [11]. Selectin expression is induced by inflammatory and locally produced chemokines. P-selectin is rapidly translocated from intracellular deposits to the cell membrane, whereas E-selectin is transcriptionally regulated [15].

The tetrasaccharide CD15s is a mutual ligand for E- and P-selectin although with a higher affinity to E-selectin [16, 17]. CD15s is a terminating oligosaccharide of O-glycans, N-glycans or glycosphingolipids, which are expressed by leukocytes or tumor cells [18]. The first step of interaction between leukocytes and EC is mediated by E- and P-selectin on EC. As we hypothesize that RASF use the molecules of the leukocyte adhesion cascade, we evaluated whether RASF interact with selectins and other adhesion molecules under dynamic and static conditions and whether these interactions include CD15s.

RESULTS

RASF-adhesion towards EC: static conditions

Calcein-AM-stained SF cultured in RPMI or DMEM with comparable supplements and non-stained primary EC or HUVEC with/without prior TNF-activation were used (Fig.1A). Strongest adherence was observed in RPMI-cultured RASF towards TNF-activated HUVEC (2.25-fold±0.41, Fig.1B) compared to DMEM-cultured RASF towards non-activated HUVEC (set to 1, $P = 0.2277$, n = 3 each). Adhesion of RPMI-cultured RASF was higher compared to RPMI-cultured OASF towards activated HUVEC. RPMI-cultured OASF towards TNF-activated HUVEC only showed a 1.13-fold±0.14 increase ($P > 0.999$) compared to DMEM-cultured OASF towards non-activated HUVEC (set to 1). When comparing RASF-adhesion towards isolated human venous and arterial EC, RASF-adhesion was higher in both, arterial and venous EC when cultured in RPMI compared to DMEM (arterial $P = 0.0186$, venous $P = 0.0078$, Fig.1C). In addition, RASF adhesion was higher when using venous EC compared to arterial EC in RPMI ($P = 0.0119$), which were selected for further experiments (Fig.1C).

Inhibition of VCAM-1 as well as E-selectin (A-205804) or using the proteasome inhibitor Bortezomib did not inhibit cell-to-cell adhesion in the absence (vs. control: anti-VCAM-1 1.30-fold, A-205804 1.91-fold, Bortezomib 3 nM 1.18-fold, 6 nM 0.98-fold) or presence of TNF (vs TNF-stimulated control: anti-VCAM-1 1.19-fold, A-205804 1.69-fold, Bortezomib 3 nM 1.03-fold, 6 nM 1.04-fold).

RASF-adhesion towards EC: flow conditions

SF-attachment towards E-selectin and P-selectin was evaluated in flow-chamber assays (Fig.2A). First, RPMI and DMEM medium was compared in the flow assay using E-selectin coated capillaries. Similar to the static adhesion assay, the number of adhering and rolling fibroblasts was very low when using DMEM. Primary venous EC and HUVEC led to comparable findings regarding cell numbers. Therefore, RPMI medium and HUVEC were used for further flow experiments. FCS-coated (negative control) and P-selectin coated channels showed no to very low RASF-rolling or -adhesion to the channel surface (n = 10; Table1, Fig.2B). RASF showed rolling and/or adhering to E-selectin in all settings (n = 10; Table 1) significantly higher than to P-selectin (n = 10; Table 1). In contrast to RASF, OASF showed lower rolling/adhesion capability to E-selectin (0.5 dyn cm^{-2}: P = 0.0010; 0.9 dyn cm^{-2}: P = 0.0828; 1.8 dyn cm^{-2}: P = 0.9999; n = 10; Table 1). Similar to RASF, interactions of OASF with FCS as well as P-selectin was 0 in all settings (n = 10).

RASF were able to adhere to and roll onto TNF-activated HUVEC (n = 6; Table 1, Fig.2C). Adhesion of RASF towards and rolling on EC was higher in activated EC compared to non-activated EC (n = 6; Table 1). OASF showed lower interaction with activated or non-activated EC compared to RASF (n = 6, Table 1). As control, the use of an E-selectin ab resulted in a significant decrease of RASF adhesion to TNF-activated EC (0.5 dyn cm^{-2} 25.83±4.07 vs. 14.5±2.47, n = 6). Interestingly, OASF showed comparable adhesion towards activated and non-activated EC. Of note, EC were cultured to 100% confluency under flow conditions (Fig.2D). Comparative analysis showed that there was no difference whether EC were precultured under flow or static conditions (data not shown).

CD15s-expression on RASF

As different cells such as EC, leukocytes and RASF are cultured in different media, their effect (comparable supplements) as well as of RA, OA and healthy serum on CD15s-expression on SF was evaluated and quantified (Fig.3A,B). RA serum showed the strongest induction on CD15s-expression by RASF, lower CD15s signals were observed with OA and healthy serum (Fig.3B). Compared to CD15s-induction with sera, the effect of medium was low. DMEM did not significantly induce CD15s-expression on SF but was visible in RPMI-cultured RASF (Fig.3A,B). OASF showed a lower induction of CD15s with RA serum and RPMI then RASF (Fig.3A). Signal quantification showed that CD15s induction was significantly higher with RA serum compared to OA serum (P = 0.0093) and serum from healthy donors (P = 0.0044) in RASF as well as for OASF (P = 0.0152 and P = 0.0008, respectively; Fig.3B). CD15s signals were higher in RA- and OASF cultured in RPMI compared to DMEM and significant for OASF (OASF RPMI vs. DMEM P = 0.0437) (Fig.3B). To further characterize the factors within the RA serum involved in CD15s induction, RASF were stimulated with 10 or 50 ng mL^{-1} TNFα or 10 ng mL^{-1} IL-1β. Both factors induced CD15s expression with TNFα (both concentrations) being more potent compared to IL-1β. Of note, TNF-induced CD15s was observed in both, DMEM as well as in RPMI cultured RASF compared to the unstimulated control (Fig.3C).

Vimentin/CD15s double-positive cells in RA synovium

In RA synovium (n = 15), 53% of tissues expressed CD15s detectable in lining layer and sublining (Fig.4A). As expected, CD15s was especially detectable close to inflammatory cell infiltrates. To confirm that the E-/P-selectin ligand CD15s is not only expressed on RASF *in vitro*, immunofluorescence double-staining of RA tissues for vimentin (antibody against a mesenchymal marker leading to strong signals in fibroblasts, but weak signals e.g. in leukocytes [19]) with CD15s were evaluated (Fig.4B). RA tissues selected for fluorescence double-staining (n = 12) were CD15s-positive: 4/12 RA tissues (33%) showed no colocalization of CD15s with vimentin. 8/12 tissues

showed CD15s/vimentin double-stained cells (67%). Of those, 4/8 showed CD15s-positive mesenchymal cells solely within sublining (50%). In 2/8 tissues CD15s-expressing cells were detectable within or close to vessels and within sublining (25%). In 2/8 tissues double-stained cells solely close to or within vessels were detectable (25%). In OA tissues (n = 7) no double-staining was detectable (not shown). CD15s-staining was additionally compared to CRP serum levels of the respective patients (Fig.4C). CRP and CD15s correlation showed increased CRP-levels in CD15s-expressing tissues (r = 0.415, mean CRP with CD15s-positive cells: 4.33±0.83 mg dL^{-1}; RA patients without CD15s: 2.03±1.21 mg dL^{-1}). All RA patients were female. CD15s signal was independent of age (mean age 64±7.01) and treatment (biologics, MTX, glucocorticoids). 4/5 CD15s positive RA patients and 3/7 CD15s negative RA patients were rheumatoid factor positive. The rheumatoid factor titer did not correlate with CD15s expression.

E-/P-selectin-deficiency effects on RASF-migration in SCID-mice

The effects of selectins on RASF-invasion into directly coimplanted cartilage and migration to contralaterally inserted cartilage (without RASF) was evaluated in E-/P-selectin deficient compared to E-/P-selectin-competent wildtype SCID-mice. At the ipsilateral implantation site (cartilage with RASF), invasion scores for E-/P-selectin competent as well as deficient animals were comparable 45 days post-implantation (E-/P-competent 1.85±0.54 vs E-/P-deficient 1.81±0.40 P = 0.301). In the E-/P-competent SCID-mouse control setting, there was no significant difference between primary and contralateral RASF-mediated cartilage invasion (E-/P-competent ipsilateral 1.85±0.54 vs. contralateral 2.11±0.49). However, the RASF-mediated cartilage invasion was significantly reduced at the contralateral site (cartilage implanted without RASF) of E-/P-deficient animals compared to the E-/P-competent implants (E/P-deficient contralateral 1.19±0.61 vs. E-/P-competent: 2.11±0.49, P = 0.023, Fig.5A). After 60 days, the reduced RASF-invasion in contralateral implants of E-/-P-selectin-deficient animals compared to E-/P-competent animals was still visible but not significant (P = 0.065)

due to the accumulation of cartilage-invading RASF over time (E-/P-competent, ipsilateral: 1.99±0.56, contralateral: 1.79±0.83 vs. E-/P-deficient, ipsilateral: 1.78±0.96, contralateral: 1.22±0.73; Fig.5B). The effect of the proteasome-inhibitor Bortezomib, known to reduce adhesion molecule expression (e.g. integrins), was evaluated. Invasion was comparable for saline as well as Bortezomib treated animals at the ipsilateral (saline 1.05±0.54, Bortezomib 0.89±0.40) and contralateral site (saline 1.67±0.84, Bortezomib 1.67±0.97, Fig.5C).

To confirm that E-, P-selectin and VCAM-1 are present in wildtype SCID-mouse implants, LMM to isolate murine EC was performed with subsequent realtime-PCR. All adhesion molecules were expressed within the implants on mRNA level (Fig.6A). As additional control, murine cultured EC were TNF-activated for 6 h to induce adhesion molecule expression and mRNA was used as positive control. VCAM-1 expression was also confirmed by immunohistochemistry (Fig.6B). Furthermore, the presence of human CD15s (on the implanted human RASF) was confirmed in the SCID mouse implants. Although CD15s was not detectable at the cartilage invasion zone (similar to the human synovial tissues), CD15s positive cells were detectable within the implants (Fig.6C).

DISCUSSION

Cartilage invasion by RASF can be observed very early during the disease, often starting at the boarder of the joint capsule attaching to cartilage and bone. The cells actively invading the cartilage are RASF [5, 6, 20]. A discerning feature of RA is that it can occur at multiple joints and the involvement of several joints can be explained by long-distance migration of RASF via the blood stream [1, 2]. How RASF leave the bloodstream is unknown so far. We hypothesized that they use CAM of the leukocytes adhesion cascade as could be shown for metastasizing cancer cells [8]. We evaluated the potential of RASF to interact with EC, specifically via selectins, as E-selectin is the initial binding

partner of blood-borne cells with EC in post-capillary venules [11]. Selectins are not in their active conformation below 0.5 dyn cm^{-2}. Above 1.8 dyn cm^{-2}, cells mainly flow in the center of the stream and no longer interact with EC [21]. RASF were able to adhere to E-selectin- but not P-selectin-coated capillaries to a higher degree than OASF. Due to the pre-activated state of RASF, e.g. due to epigenetic modifications and altered metabolism of RASF [3, 22, 23], they usually show a higher reactivity and matrix adhesion than OASF and an increased cartilage invasive and destructive potential. RASF-adhesion to EC was significantly higher after TNF-activation of EC. TNF induces adhesion molecules on EC [24] and TNF serum levels are increased in RA [25]. E-selectin is transcriptionally regulated and present on EC after few hours of EC activation [15]. Flow-adhesion experiments using tumor cells showed similar results comparable to ours with RASF [9]. Although paravasation of leukocytes also involves binding to P-selectin [26], this seems not to be the case for RASF.

The next step of leukocyte/EC-interaction is adhesion of integrins and members of the immunoglobulin superfamily [11]. In contrast to selectins, these adhesion molecules bind under static as well as flow conditions [9]. The increased adhesion of RASF to EC compared to OASF under static conditions (selectin-independent) was confirmed in cell-to-cell-binding assays. Specifically, culture in RPMI (generally used for culture of blood-derived cells and containing e.g. more vitamins, amino acids and iron in comparison to DMEM, representing a more basic medium) and TNF-activated venous EC yielded strong RASF-adhesion to EC. As the leukocyte adhesion cascade takes place in post-capillary venules [27], similar mechanisms seem to be used by RASF. In RA synovium, VCAM-1, which binds to VLA-4 [28, 29], is increased [28] and expressed by SF and EC, allowing tight adhesion between cells. The role of VCAM-1 could already be shown by the use of anti-VCAM-1-antibodies, which reduced RASF-adhesion [1].

CD15s, a binding partner of E-selectin, is relevant in tumor cell/EC interactions [30, 31]. Two thirds of RA tissues demonstrated colocalisation of CD15s and vimentin in large cells of mesenchymal origin with strong vimentin-signal (most likely of fibroblastic origin, as other vimentin-positive cells display weaker vimentin-signals) in close proximity or even within blood vessels of some tissues. Although vimentin is not solely expressed by fibroblasts, at least the presence of mesenchymal cells with strong vimentin signal [19] expressing CD15s and their location would be compatible with the presence of migrating RASF in RA tissue. CD15s-expression could be confirmed on RASF *in vitro* and was especially increased by culture especially in RA serum and higher on RASF than OASF. CD15s is expressed e.g. by T cells, monocytes, follicular dendritic cells and different tumor cells [30, 32-34]. As RASF may migrate within the blood stream and the conditions in the blood induces CD15s-expression on RASF, this potentially allows the binding of RASF to activated EC and, therefore, the ability for RASF to leave the circulation. Additionally, the amount of CD15s-positive cells correlated with CRP levels confirming that inflammatory environments induce CD15s expression in RASF.

E-/P-selectin-deficient SCID-mice confirmed that after 45 days a significantly reduced number of RASF arrive and invade the contralateral cartilage compared to wildtype SCID-mice. The presence of murine E-, P-selectin and VCAM-1 in vessels grown beside or inside implants in E-/P-competent mice was confirmed. However, after 60 days, contralateral invasion was comparable showing that compensatory mechanisms via other adhesion molecules may be active [35] or sufficient cells arrive at the contralateral site (as migration was not completely inhibited) to reach maximum invasion. Interestingly, mainly long-distance but not local migration was affected. The proteasome inhibitor Bortezomib A is a substance used in tumor therapy [36]. Proteasomes are cellular complexes that degrade proteins. In normal cells, proteasomes regulate protein levels by degradation of ubiquitinylated proteins and removal of abnormal or misfolded proteins. In some malignancies, proteins that normally kill cancer cells are rapidly removed. Proteasome inhibitors suppress the

protein breakdown and, therefore, those proteins are able to eliminate the cancer cells, e.g. as demonstrated in multiple myeloma. In addition, proteasome inhibition has been discussed to prevent the breakdown of pro-apoptotic factors [37]. RASF are known to have an increased resistance to apoptosis and increased survival [38]. Therefore, we evaluated the effect of Bortezomib on RASF in the SCID mouse model. RASF-mediated cartilage invasion at the ipsilateral site (cartilage implanted with RASF) and at the contralateral site (cartilage implanted without RASF) was not altered by Bortezomib suggesting that inhibition of proteasome activity, potentially affecting apoptosis and RASF survival, does not play a crucial role in this system. However, although the mean invasion scores at the ipsilateral and contralateral site were similar with and without Bortezomib, the variability of the invasion score in this model is high, specifically in this setting due to the limited number of implants. The high variability of the data impairs the ability to have a conclusive interpretation and thus further investigation will be required.

Current treatment strategies -in part very successfully used for RA treatment although not all patients respond sufficiently- mainly target the (auto-)inflammation. Inhibition of cytokines such as TNF and IL-6 as well as B-cells and recently intracellular kinases are established therapies for RA. Although the reduced inflammatory milieu also reduces the activation of RASF, cartilage invasion can be slowed down but usually not completely stopped. To develop a strategy directly inhibiting RASF invasion and their increased migratory potential could therefore benefit the patients in the long term.

Our data indicate that the milieu within vessels induces E-selectin ligand expression on RASF, which enables RASF to interact with E-selectin on EC under flow conditions at distant sites. The identification of the target molecules responsible for the spreading of RASF may open up new avenues for RA therapy by targeting this adhesion cascade in order to slow RA progression. Notably, corticosteroids were shown to downregulate E-selectin expression in EC and our finding of the

importance of E-selectin in RASF-adhesion could explain in part why corticosteroids are successful in slowing down RA progression.

METHODS

Cells and tissues

RA and OA synovium, bone fragments and cartilage were obtained during knee replacement surgeries (Agaplesion-Markus-Krankenhaus). Patients fulfilled classification criteria of the American College of Rheumatology [39-41]. Human arteries and veins were obtained (Vascular and Cardiac Surgery, Kerckhoff-Klinik). The study was approved by the local ethics committee (Justus-Liebig-University Giessen) and all patients gave written informed consent.

Synovium samples were snap frozen and remaining tissue digested (Dispase-II-solution, 0.1 mL stock solution mL^{-1}, PAN-Biotech, Aidenbach, Germany) [42] and passed through cell strainers. SF were cultured in DMEM (PAA-Laboratories, Cölbe, Germany) containing 10% fetal calf serum (FCS, Sigma-Aldrich, Taufkirchen, Germany), 1 U mL^{-1} penicillin/streptomycin and 1mM HEPES (PAA-Laboratories) [42, 43]. Normal human cartilage (macroscopically intact surface and normal histological structure) was cut [44] and in part snap frozen for hematoxylin/eosin staining (H/E).

The vessel lumen was washed twice, filled with collagenase H and ligated. After 1 h at 37°C, the EC-containing solution was mixed 1:4 with supplemented DMEM (20% FCS, 1 U mL^{-1} penicillin/streptomycin, 1 mM HEPES). After centrifugation, cells were resuspended in supplemented DMEM with 0.1 mg mL^{-1} EC growth supplement (BD Biosciences, Heidelberg, Germany) and transferred to rat tail collagen-coated wells. The next day, adherent cells were washed. Medium was changed every 2-3 days for up to 3 passages to avoid dedifferentiation. Solely EC cultures without fibroblast contamination (vimentin/CD31 immunocytochemical confirmation) were used. At 100% confluency, cells were detached, centrifuged and placed in rat tail collagen-coated plates. HUVEC

(Promocell, Heidelberg, Germany) were cultured on uncoated plates with EC Growth-Medium 2 (Promocell) for up to 2 passages.

CD15s Induction

$1.5x10^4$ SF in supplemented DMEM were added to chamber slides. After 24 h, cells from RA and OA patients were washed and supplemented DMEM, RPMI for 48 h, respectively. In addition, serum from healthy donors, RA and OA patients (n = 10) was added for 48 h in parallel to the culture in medium. In addition, IL-1β and TNFα (R&D Systems) were added to RASF in DMEM due to the increased concentrations of these cytokines in the RA serum used. Cells were washed and immunohistologically stained for CD15s.

Immunohistochemical/-fluorescent staining

5 µm sections or chamber slides were incubated with anti-human CD15s-antibodies (Sialyl-Lewis-X, BD Bioscience) and anti-human or -murine CD62E (E-selectin, Abcam, Cambridge, UK). As secondary antibody, the Histofine Simple-Stain MAX-PO kits (Nichirei Biosciences, Tokyo, Japan) and for color development Peroxidase-Substrate kits (AEC, Vector-Laboratories, Grünberg, Germany) were used. Red signals were quantified (images with similar recording parameters, ImageJ 1.32 open-source software) for each biological replicate means of three representative areas, each were calculated and used for statistics. Fluorescent staining was performed using anti-human CD15s (BD Bioscience) and vimentin (Dako, Hamburg, Germany) antibodies. The used anti-vimentin-antibody stained fibroblast-like cells strongly whereas leukocytes and other vimentin positive cells displayed weak vimentin signals [19]. Secondary antibodies used in double stainings against CD15s-antibodies were FITC-labeled (BD-Bioscience), against vimentin-antibodies Cy3-labeled (Abcam). For

immunofluorescence of human CD15s in SCID mouse implants, CD15s antibodies were Alexa Fuor®647 labeled with mouse IgMκ as control (563526, 560806; BD Pharmingen).

Cell-to-cell-binding assay

RASF were Calcein-AM stained (living cells: green fluorescence) for 30 min. Cells were detached with accutase and centrifuged. $5x10^3$ cells were added to confluent EC-layers and incubated for 1 h at 37°C. EC were pretreated for 24 h with the E-selectin inhibitor A-205804 (S2885, Selleckchem) or the blocking anti-human VCAM1 antibody (clone BBIG-V1R&D Systems) with/without 10 ng mL^{-1} TNF (R&D Systems). Bortezomib (3 nM or 6 nM) was added 2 h before cell-cell-adhesion with/without 10 ng mL^{-1} TNF. Supernatants were removed, replaced with serum-free medium and shaked for 5 min full speed twice to remove loosely attached RASF. Attached fluorescent fibroblasts (on non-stained EC) were quantified in four representative areas each. Using bright field microscopy, confluency of the EC layer was confirmed.

Laminar-flow assay

As previously published [9], capillary slides (µ-Slide $VI^{0.4}$, „ibidiTreat-pretreated“, Ibidi, Martinsried, Germany) were coated with 30 µl FCS, 30 µl recombinant human E-selectin (1 mg mL^{-1} E-Selectin/Fc-Chimera, 1:20 in PBS) or P-selectin (100 µg mL^{-1} P-Selectin/Fc-Chimera, 1:2 in PBS, R&D Systems) for 1 h at room temperature or $1.35x10^4$ HUVEC were added into capillary slides and grown to confluency overnight at 37°C/10% CO_2. Next day, EC layers were incubated under dynamic flow (2 dyn cm^{-2} 60min, 5 dyn cm^{-2} 60min, then 10 dyn cm^{-2}) using the Ibidi Pump-System (Ibidi). EC visibly arranged themselves into the flow direction. HUVEC were/were not activated for 6 h with 10 ng mL^{-1} TNF (R&D Systems) in EC Growth Medium 2. $2x10^6$ SF cultured in supplemented DMEM or RPMI were transferred into a syringe pump (Model-100-Series, kdScientific, Holliston, USA) and connected

to the capillary slide. SF migration through capillaries was monitored microscopically. Cells slowly rolling over the surface and arrested cells were quantified. Means of rolling/arresting cells per visual field were calculated for each recorded sequence (1 min each). Flow rates were 18.4 mL h^{-1} / 30.5 mL h^{-1} / 60.5 mL h^{-1} resulting in shear stress of 0.5 dyn cm^{-2} / 0.9 dyn cm^{-2} / 1.8 dyn cm^{-2}, representing rates detected in post-capillary venules.

Laser-mediated-microdissection (LMM) and realtime-PCR

LMM was performed as previously described [45]. Vessels containing EC (10.000 per implant) were cut and the 5 µm frozen sections of SCID-mouse implants were placed on PEN-membrane coated slides (P.A.L.M., Bernried, Germany). After fixing, nuclei were hematoxylin-stained and water was removed (twice each for 2 min: 70% / 96% / 100% ethanol). Sections were dried and immediately used or stored at -80°C (maximum 2 days). LMM was performed using a P.A.L.M MicroBeam-C system, selected areas cut and catapulted into adhesive caps (P.A.L.M.) containing 10 µl RNA extraction buffer. RNA was isolated using the RNeasy Mini Kit (Qiagen). RNA was reverse-transcribed (AMV reverse transcriptase, Promega) using random-hexamer primers (Roche, Mannheim, Germany): denaturation (2 min 70°C), 30 min 42°C, 30 min 55°C, 10 min 70°C. Realtime-PCR was performed using a LightCycler (Roche) [45-47]. The SYBR-Green-system (Absolute SYBR-Capillary Mix, Thermo-Fisher Scientific, Dreieich, Germany) was used (supplementary table 1) with 18S rRNA for normalization, finished by melting curve analysis.

SCID-mouse-model

18 female, six weeks old Crl-scidBR mice (Charles River, Sulzbach, Germany) and 14 male plus 4 female SCID-select-mice (SCID-Select-mice $E^{-/-}/P^{-/-}$) characterized by [7] (kindly provided by Prof. Udo Schumacher, Hamburg) were kept under pathogen-free conditions

with water and food *ad libitum*. Animals underwent inverse-wrap implantation surgery [44] with subcutaneous implantation of $1.5x10^5$ RASF together with healthy human cartilage in a carrier matrix (Gelfoam, Pfizer, New York, USA) at the ipsilateral site. Contralaterally, cartilage in a carrier matrix without RASF was implanted [1, 2]. SCID-mice were scarified after 45 or 60 days, implants removed, snap frozen, cut into 5 µm sections, stained (H/E) and scored [1, 2, 44]. Six wildtype SCID mice were treated with Bortezomib (1 µg g^{-1}) at day 1, 3, 6, 10 and 14 followed by a 10-day break comparable to application in humans (control: saline).

Statistics

Values presented as mean±standard deviation (SD). Means of experimental replicates were calculated and the mean for each biological replicate used for statistics. For non-normally distributed data, a Kruskal-Wallis test with Dunn's multiple comparison test was used for unpaired data and the Friedmann test with Dunn's multiple comparison test for paired data. The Wilcoxon signed rank test with Bonferroni correction was used for paired data when the number of data pairs was not equal across all data sets. For normally distributed data, ANOVA and Sidak's multiple comparison test was used. *$P < 0.05$, **$P < 0.01$, ***$P < 0.001$.

FUNDING: This study was supported by the Federal Ministry of Education and Research (BMBF) as a part of the project IMPAM (01EC1008G), the excellence cluster for cardiopulmonar research (ECCPS) and by the Kerckhoff-Stiftung.

ACKNOWLEDGMENTS: We thank Carina Schreiyäck for excellent technical support during the revision of the manuscript.

CONFLICT OF INTERESTS: The authors declare no conflict of interest. Study sponsors were not involved in the study design, collection, analysis and interpretation of data, in the writing of the manuscript, and in the decision to submit the manuscript for publication.

REFERENCES

1. Lefevre S, Knedla A, Tennie C *et al.* Synovial fibroblasts spread rheumatoid arthritis to unaffected joints. *Nat Med* 2009; **15:** 1414-1420.

2. Neumann E, Lefevre S, Zimmermann B *et al.* Migratory potential of rheumatoid arthritis synovial fibroblasts: additional perspectives. *Cell Cycle* 2010; **9:** 2286-2291.

3. Doody KM, Bottini N, Firestein GS. Epigenetic alterations in rheumatoid arthritis fibroblast-like synoviocytes. *Epigenomics* 2017; **9:** 479-492.

4. Ley K. The role of selectins in inflammation and disease. *Trends Mol Med* 2003; **9:** 263-268.

5. Neumann E, Lefevre S, Zimmermann B *et al.* Rheumatoid arthritis progression mediated by activated synovial fibroblasts. *Trends Mol Med* 2011; **16:** 458-468.

6. Korb-Pap A, Bertrand J, Sherwood J *et al.* Stable activation of fibroblasts in rheumatic arthritis-causes and consequences. *Rheumatology (Oxford)* 2016; **55:** ii64-ii67.

7. Köhler S, Ullrich S, Richter U *et al.* E-/P-selectins and colon carcinoma metastasis: first in vivo evidence for their crucial role in a clinically relevant model of spontaneous metastasis formation in the lung. *Br J Cancer* 2010; **102:** 602-609.

8. Langley RR, Fidler IJ. Tumor cell-organ microenvironment interactions in the pathogenesis of cancer metastasis. *Endocr Rev* 2007; **28:** 297-321.

9. Richter U, Schroder C, Wicklein D *et al.* Adhesion of small cell lung cancer cells to E- and P-selectin under physiological flow conditions: implications for metastasis formation. *Histochem Cell Biol* 2011; **135:** 499-512.

10. McEver RP, Zhu C. Rolling cell adhesion. *Annu Rev Cell Dev Biol* 2010; **26:** 363-396.

11. Ley K, Laudanna C, Cybulsky MI *et al.* Getting to the site of inflammation: the leukocyte adhesion cascade updated. *Nat Rev Immunol* 2007; **7:** 678-689.

12. Lawrence MB, Kansas GS, Kunkel EJ *et al.* Threshold levels of fluid shear promote leukocyte adhesion through selectins (CD62L,P,E). *J Cell Biol* 1997; **136:** 717-727.

13. Yago T, Wu J, Wey CD *et al.* Catch bonds govern adhesion through L-selectin at threshold shear. *J Cell Biol* 2004; **166:** 913-923.

14. Varki A. Selectin ligands. *Proc Natl Acad Sci U S A* 1994; **91:** 7390-7397.

15. Somers WS, Tang J, Shaw GD *et al.* Insights into the molecular basis of leukocyte tethering and rolling revealed by structures of P- and E-selectin bound to SLe(X) and PSGL-1. *Cell* 2000; **103:** 467-479.

16. Pan LH, Yamauchi K, Sawai T *et al.* Inhibition of binding of E- and P-selectin to sialyl-Lewis X molecule suppresses the inflammatory response in hypersensitivity pneumonitis in mice. *Am J Respir Crit Care Med* 2000; **161:** 1689-1697.

17. Norman KE, Anderson GP, Kolb HC *et al.* Sialyl Lewis(x) (sLe(x)) and an sLe(x) mimetic, CGP69669A, disrupt E-selectin-dependent leukocyte rolling in vivo. *Blood* 1998; **91:** 475-483.

18. Barthel SR, Gavino JD, Descheny L *et al.* Targeting selectins and selectin ligands in inflammation and cancer. *Expert Opin Ther Targets* 2007; **11:** 1473-1491.

19. Giorno R, Sciotto CG. Use of monoclonal antibodies for analyzing the distribution of the intermediate filament protein vimentin in human non-Hodgkin's lymphomas. *Am J Pathol* 1985; **120:** 351-355.

20. Ospelt C. Synovial fibroblasts in 2017. *RMD Open* 2017; **3:** e000471.

21. Beste MT, Hammer DA. Selectin catch-slip kinetics encode shear threshold adhesive behavior of rolling leukocytes. *Proc Natl Acad Sci U S A* 2008; **105:** 20716-20721.

22. Bustamante MF, Garcia-Carbonell R, Whisenant KD *et al.* Fibroblast-like synoviocyte metabolism in the pathogenesis of rheumatoid arthritis. *Arthritis Res Ther* 2017; **19:** 110.

23. Frank-Bertoncelj M, Klein K, Gay S. Interplay between genetic and epigenetic mechanisms in rheumatoid arthritis. *Epigenomics* 2017; **9:** 493-504.

24. Mackay F, Loetscher H, Stueber D *et al.* Tumor necrosis factor alpha (TNF-alpha)-induced cell adhesion to human endothelial cells is under dominant control of one TNF receptor type, TNF-R55. *J Exp Med* 1993; **177:** 1277-1286.

25. Ebrahimi AA, Noshad H, Sadreddini S *et al.* Serum levels of TNF-alpha, TNF-alphaRI, TNF-alphaRII and IL-12 in treated rheumatoid arthritis patients. *Iran J Immunol* 2009; **6**(3)**:** 147-53.

26. Steeber DA, Tedder TF. Adhesion molecule cascades direct lymphocyte recirculation and leukocyte migration during inflammation. *Immunol Res* 2000; **22:** 299-317.

27. He P. Leucocyte/endothelium interactions and microvessel permeability: coupled or uncoupled? *Cardiovasc Res* 2010; **87:** 281-290.

28. Lowin T, Straub RH. Integrins and their ligands in rheumatoid arthritis. *Arthritis Res Ther* 2011; **13:** 244.

29. Silverman MD, Haas CS, Rad AM *et al.* The role of vascular cell adhesion molecule 1/ very late activation antigen 4 in endothelial progenitor cell recruitment to rheumatoid arthritis synovium. *Arthritis Rheum* 2007; **56:** 1817-1826.

30. Nakamura M, Furukawa Y, Sasaki R *et al.* UDP-GlcNAc:Galbeta1-->3GalNAc (GlcNAc to GalNAc) beta1-->6N-acetylglucosaminyltransferase holds a key role on the control of CD15s expression in human pre-B lymphoid cell lines. *Glycobiology* 1999; **9:** 1-12.

31. Paganuzzi M, Bobbio B, Marroni P *et al.* Prognostic role of serum sialyl Lewisx (CD15s) in colorectal cancer. *Oncology* 2003; **65:** 52-59.

32. Sbrana S, Buffa M, Bevilacqua S *et al.* Granulocyte- and monocyte-platelet adhesion index in coronary and peripheral blood after extracorporeal circulation and reperfusion. *Cytometry B Clin Cytom* 2007; **72:** 215-222.

33. Suzuki A, Yamakawa M, Tsukamoto M. The adhesion molecules, l-selectin and sialyl lewis x, relate to the formation of the follicular dendritic cell-lymphocyte cluster in the mantle zone. *Immunol Lett* 2001; **79:** 181-187.

34. St Hill CA, Baharo-Hassan D, Farooqui M. C2-O-sLeX glycoproteins are E-selectin ligands that regulate invasion of human colon and hepatic carcinoma cells. *PLoS One* 2011; **6:** e16281.

35. Schwankhaus N, Gathmann C, Wicklein D *et al.* Cell adhesion molecules in metastatic neuroblastoma models. *Clin Exp Metastasis* 2014; **31:** 483-496.

36. Read MA, Neish AS, Luscinskas FW *et al.* The proteasome pathway is required for cytokine-induced endothelial-leukocyte adhesion molecule expression. *Immunity* 1995; **2:** 493-506.

37. Reece DE, Sullivan D, Lonial S *et al.* Pharmacokinetic and pharmacodynamic study of two doses of bortezomib in patients with relapsed multiple myeloma. *Cancer Chemother Pharmacol* 2011; **67:** 57-67.

38. Janczi T, Beate BB, Fehrl Y *et al.* ADAM15 in apoptosis resistance of synovial fibroblasts: converting Fas/CD95 death signals into the activation of pro-survival pathways by calmodulin recruitment. *Arthritis Rheumatol* 2018 [Epub ahead of print].

39. Altman R, Asch E, Bloch D *et al.* Development of criteria for the classification and reporting of osteoarthritis. Classification of osteoarthritis of the knee. Diagnostic and Therapeutic Criteria Committee of the American Rheumatism Association. *Arthritis Rheum* 1986; **29:** 1039-1049.

40. Taylor W, Gladman D, Helliwell P *et al.* Classification criteria for psoriatic arthritis: development of new criteria from a large international study. *Arthritis Rheum* 2006; **54:** 2665-2673.

41. Aletaha D, Neogi T, Silman AJ *et al.* 2010 rheumatoid arthritis classification criteria: an American College of Rheumatology/European League Against Rheumatism collaborative initiative. *Ann Rheum Dis* 2010; **69:** 1580-1588.

42. Neumann E, Judex M, Kullmann F *et al.* Inhibition of cartilage destruction by double gene transfer of IL-1Ra and IL-10 involves the activin pathway. *Gene Ther* 2002; **9:** 1508-1519.

43. Zimmermann-Geller B, Koppert S, Fischer S *et al.* Influence of Extracellular RNAs, Released by Rheumatoid Arthritis Synovial Fibroblasts, on Their Adhesive and Invasive Properties. *J Immunol* 2017; **197:** 2589-2597.

44. Judex M, Neumann E, Fleck M *et al.* "Inverse wrap": an improved implantation technique for virus-transduced synovial fibroblasts in the SCID mouse model for rheumatoid arthritis. *Mod Rheumatol* 2001; **11:** 145-150.

45. Hashimoto A, Tarner IH, Bohle RM *et al.* Analysis of vascular gene expression in arthritic synovium by laser-mediated microdissection. *Arthritis Rheum* 2007; **56:** 1094-1105.

46. Frommer KW, Zimmermann B, Meier FM *et al.* Adiponectin-mediated changes in effector cells involved in the pathophysiology of rheumatoid arthritis. *Arthritis Rheum* 2010; **62:** 2886-2899.

47. Junker S, Frommer KW, Krumbholz G *et al.* Expression of adipokines in osteoarthritis osteophytes and their effect on osteoblasts. *Matrix Biol* 2017; **62:** 75-91.

TABLES

Table 1: Number of adhering RASF and OASF towards E-selectin, P-selectin, and FCS coated capillaries as well as to TNFα-activated and unstimulated HUVEC under flow conditions.

		Number of adhering cells to (n=10)			Number of adhering cells to (n=6)	
		FCS	**E-selectin**	**P-selectin**	**HUVEC**	**HUVEC + TNFα**
RASF	0.5 dyn/cm^2	0	27.23±19.22	0.6±1.26	5.67±4.21	22.77±15.26
	0.9 dyn/cm^2	0	18.26±15.10	0.1±0.32	2.39±2.29	23.22±22.70
	1.8 dyn/cm^2	0	12.55±12.73	0.1±0.32	0.17±0.31	18.25±19.27
OASF	0.5 dyn/cm^2	0	11.73±7.09	0	3.39±2.65	3.33±2.14
	0.9 dyn/cm^2	0	4.07±4.51	0	1.17±1,13	1.78±1.48
	1.8 dyn/cm^2	0	1.3±1.70	0	0	0.5±0.69

LEGENDS

Figure 1: RASF adhesion under static conditions towards endothelial cells. **(a)** Example of Calcein-AM stained RASF (green fluorescence) without (left) and with TNF (middle) stimulation as well as the confluent EC layer (right, bright field, not stained). **(b)** Comparison of RASF and OASF adhesion towards non-activated or TNF-activated HUVEC cultured in DMEM or RPMI was performed. RASF cultured in RPMI showed a stronger adhesion to TNF-activated EC than DMEM cultured ones towards non-activated HUVEC (set to 1). Therefore, RPMI was selected for further experiments. Friedman test with Dunn's post-hoc/multiple comparison test was used (n = 3 biological replicates, each). **(c)** Comparison of RASF adhesion towards primary human venous endothelial (HVE, n = 8) cells and human arterial endothelial (HAE, n = 11) cells showing the strongest adhesion of RPMI-cultured RASF towards TNF-activated HVE. Therefore, venous endothelial cells were selected for further experiments (Kruskal-Wallis test with Dunn's multiple comparison was used).

Figure 2: RASF adhesion towards selectins and TNF-activated or non-activated EC. (a) Assembly of the laminar flow assay. a: syringe pump with the suspension of SF; b: chamber slides (µ-Slide VI); c: camera to record SF behaviour; d: waste container; e: computer; f: monitor with rolling SF. **(b)** Flow chamber channels were coated with E- or P-selectin. RASF (n = 10, used for each setting) flowing through the chamber showed increased rolling or attachment towards E-selectin when compared to OASF (n = 10, used for each setting) or P-selectin coating. Absolute numbers of adherent and rolling cells are shown. **(c)** RASF (n = 6) showed increased adhesion towards TNF-activated EC compared to non-activated EC as well as compared to OASF (n = 6). **(d)** EC cultured under static conditions (left) and flow conditions (right) did not influence RASF adhesion. Statistic: Friedmann test with Dunn's multiple comparison test.

Figure 3: CD15s expression under different culture conditions of RASF and OASF. (a) Highest CD15s expression was observed in RASF cultured in RA serum followed by healthy (he) serum, RPMI and DMEM (Red: CD15s). Signals for OASF were weaker compared to RASF. Scale bars: 25 µm. Red: CD15s. **(b)** Quantification of CD15s induction intensity in SF by RA, OA, and healthy serum in comparison to culture in RPMI showed the strongest induction of CD15s in SF cultured in RA serum, especially in RASF (n = 10) but also OASF (n = 10). Culture of SF in human serum led to a stronger CD15s induction compared to culture medium. ctr healthy: serum from healthy donor control. ANOVA and Sidak's multiple comparison test was used. **(c)** Addition of TNF in RPMI but also in DMEM induced comparable CD15s expression on RASF on the cell surface.

Figure 4: CD15s and vimentin-positive cells within RA synovium. (a) Expression of CD15s (red staining) in two exemplary RA synovial tissues (n = 15, 8/15 positive for CD15s). **(b)** In 4/8 CD15s-positive tissues the double stained cells were located in the synovial sublining as shown in a representative example for one RA patient (RA1). Vimentin-positive CD15s expressing cells were also detectable within the vessel lumen as shown for two examples (RA2, RA3). In some tissues, double positive cells were detectable in close proximity to vessels (RA4). Scale bars: 20 µm. Blue: DAPI stained nuclei. Red: vimentin. Green: CD15s. **(c)** When comparing the presence of CD15s stained cells with CRP levels in the patient's serum, patients with CD15s signals had higher CRP levels compared to the patients without CD15s (n = 13).

Figure 5: RASF invasion and migration in normal *versus* P- and E-selectin deficient SCID mice. (a) After 45 days, the cartilage migration to and invasion into the contralateral cartilage was significantly reduced (P = 0.023) in E-/P-selectin deficient (n = 8) compared to E-/P-selectin competent SCID mouse implants (n = 9). The cartilage-invasion of directly coimplanted RASF was comparable in E-/P-

selectin competent and deficient SCID mouse implants. **(b)** After 60 days, the difference at the contralateral site between E-/P-selectin deficient (n = 10) and competent animals (n = 11) was visible but did not reach significance (*P* = 0.065). Statistics: Wilcoxon signed rank test with Bonferroni correction was performed. **(c)** Inhibition of proteasomes in wildtype SCID-mice by Bortezomib showed comparable RASF-mediated cartilage invasion at the ipsilateral site (cartilage and RASF coimplanted) as well as at the contralateral site (cartilage implanted without RASF). n = 6 animals per group.

Figure 6: Expression of adhesion molecules on EC in SCID mouse implants. **(a)** After laser-mediated microdissection, expression analysis of murine EC out of SCID mouse implants for E-, P- selectin and VCAM-1 by realtime PCR showed the presence of all molecules within the murine endothelial cells (RNA pool of different sections, n = 10). mRNA isolated from TNF-activated cultured murine EC served as positive control. **(b)** Immunohistochemistry for VCAM1 (red staining) shows the presence of VCAM1 protein in vessels within the SCID mouse implants (implants from two different animals are shown). Blue staining: Nuclei stained with hematoxylin. **(c)** Human CD15s protein was detectable by immunofluorescence within the SCID mouse implants but not at the site of cartilage invasion. Red: CD15s, blue: nuclei with DAPI.

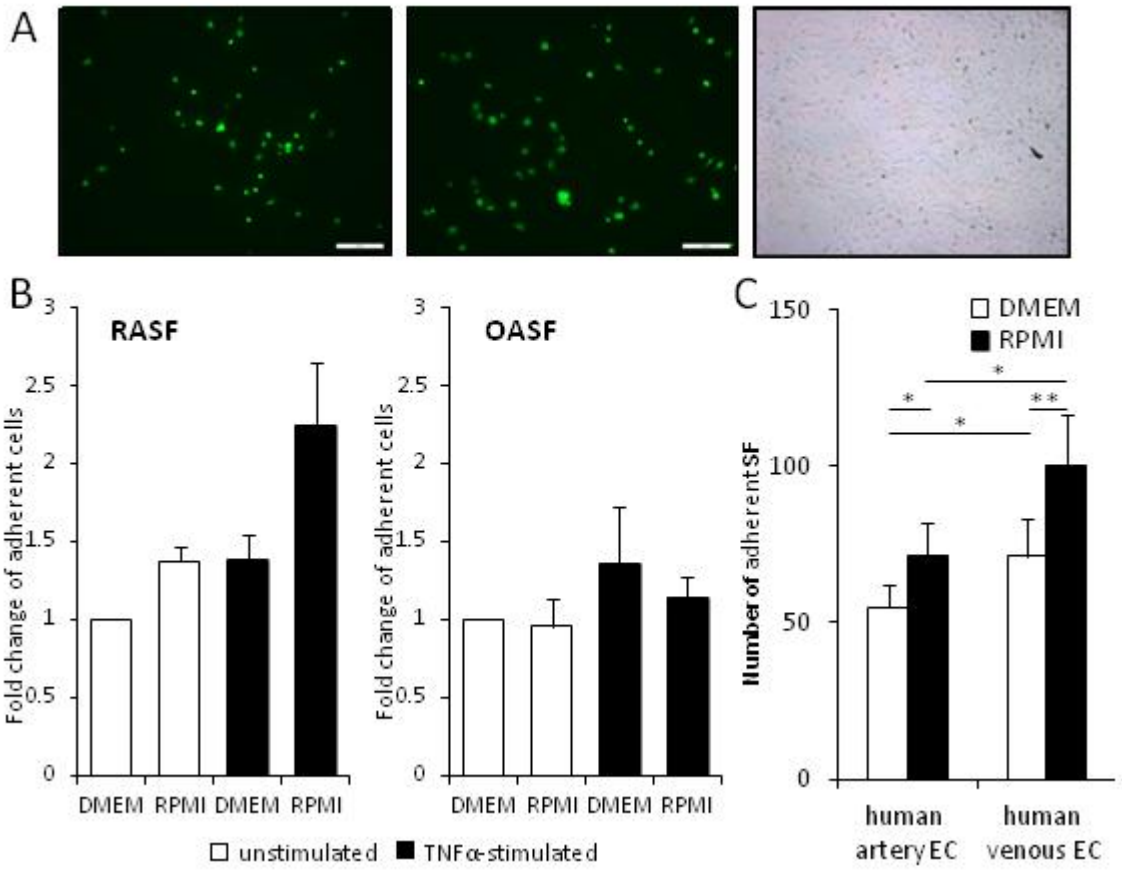

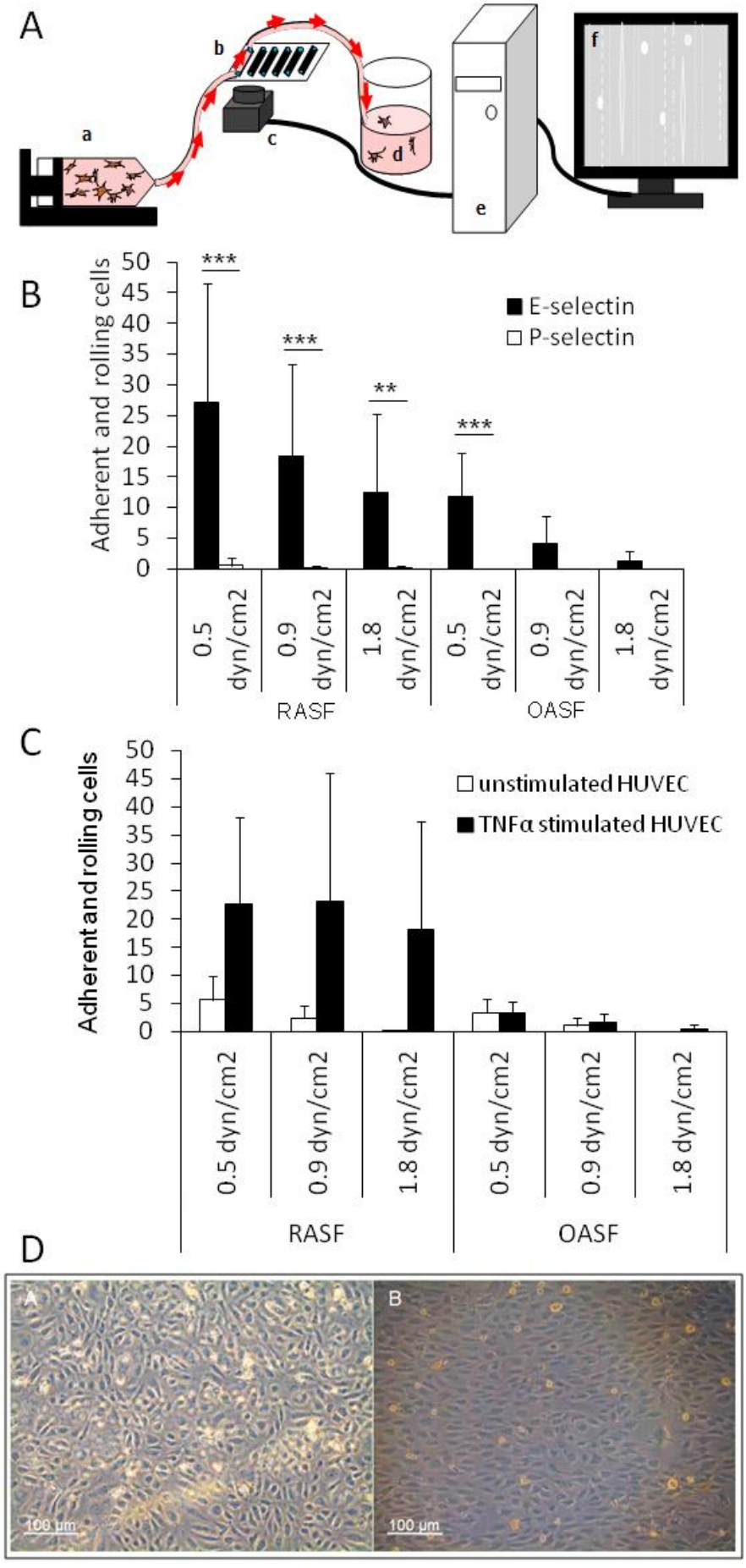

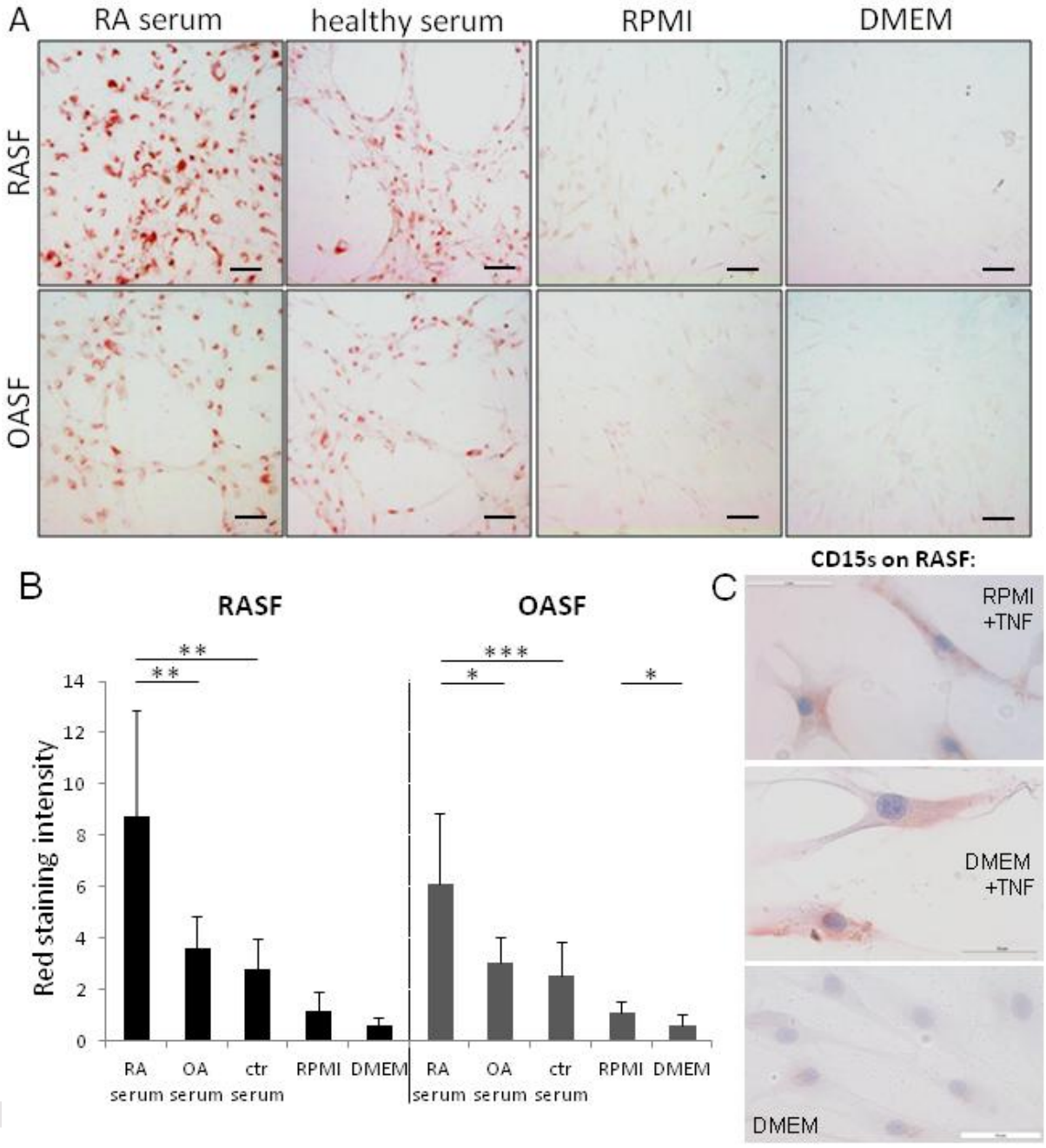

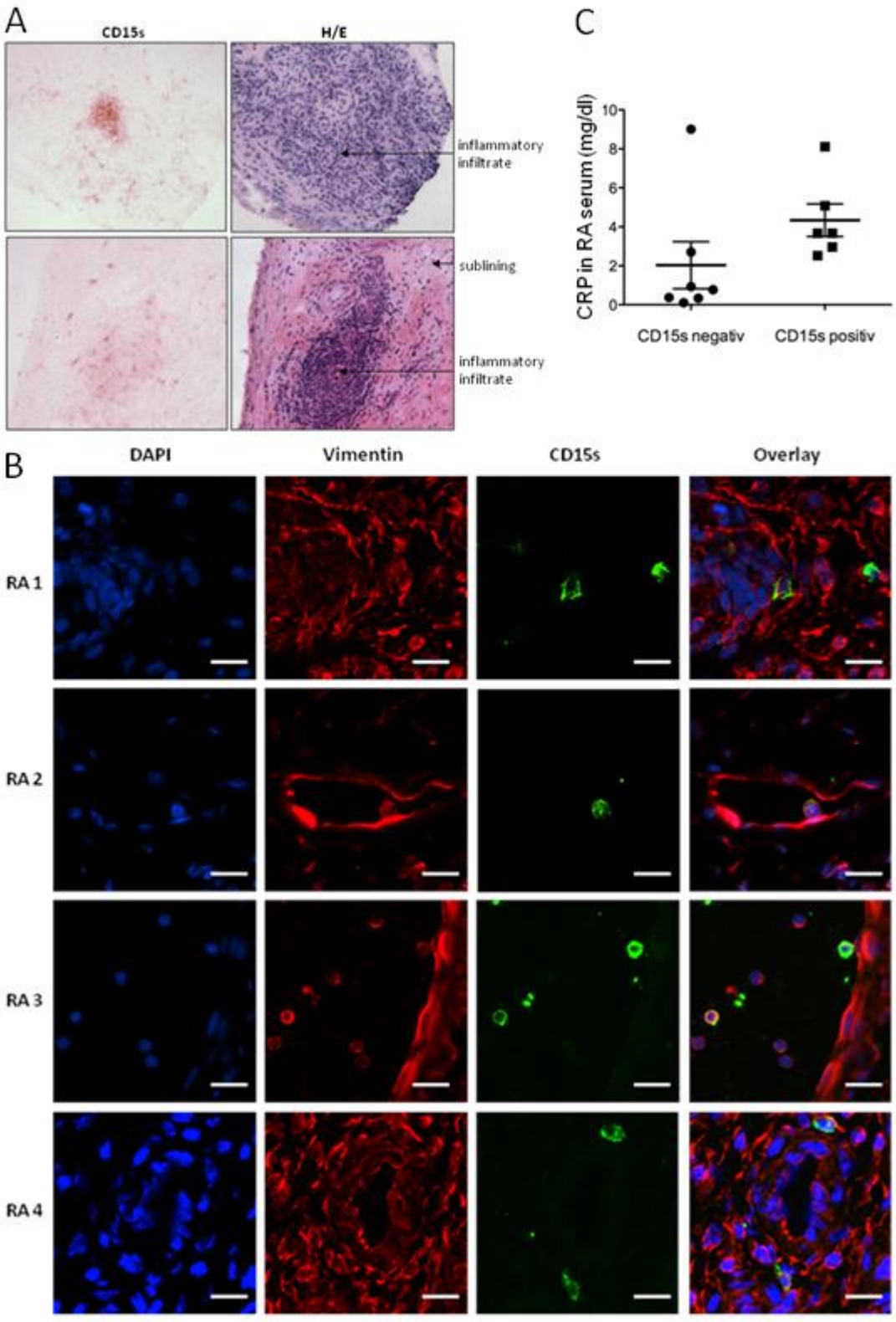

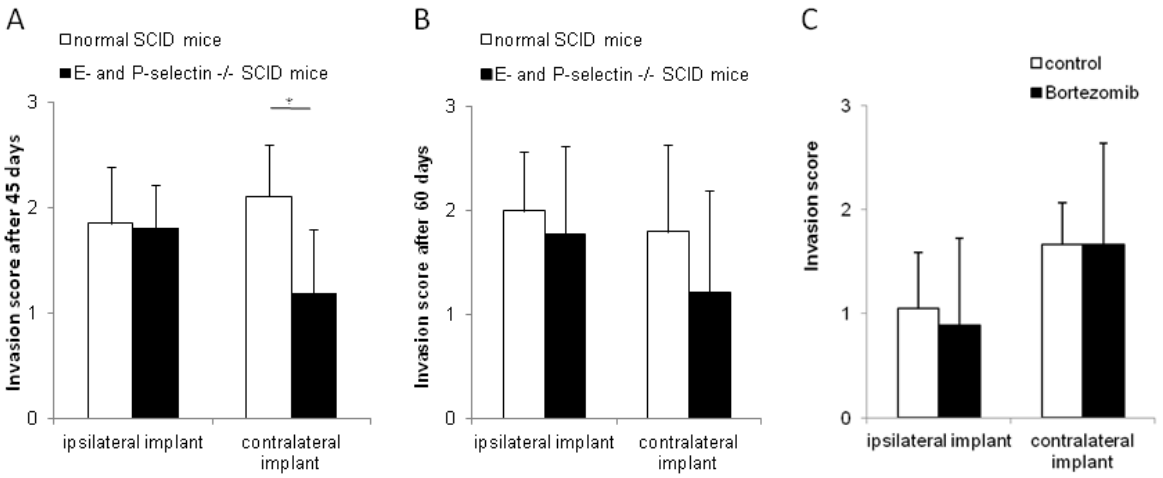

A

Adhäsion molecule	▲Ct	
	Positive control	Murine EC from implants
E-selectin	21,66	38,30
P-selectin	22,01	40,48
VCAM-1	19,18	39,81

B

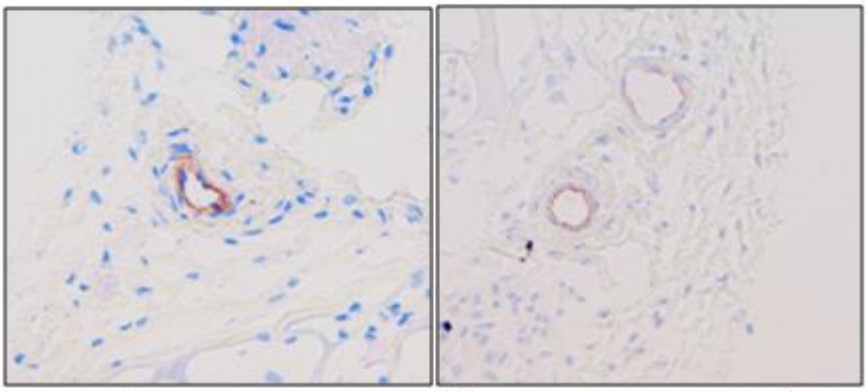

C